DOI: 10.1002/asia.201100023

1,3-Alternate Calix[4]arene as a Homobinuclear Ditopic Fluorescent Chemosensor for Ag^+ Ions

I-Ting Ho, Kuan-Chang Haung, and Wen-Sheng Chung*[a]

On the occasion of the 10th anniversary of click chemistry

Abstract: A novel 1,3-alternate calix[4]arene **L**, containing two different cationic binding sites of bis-triazoles and bis-enaminone groups, was synthesized and shown to be a homobinuclear ditopic fluorescent chemosensor for Ag^+ ions. The fluorescence intensity of **L** was selectively enhanced by binding with Ag^+ ions in methanol/chloroform (49:1, v/v) cosolvent. In the presence of most competing metal ions, **L** retains its selectivity toward Ag^+ ion. The binding constants K_1 and K_2 of the successive complexation of **L** with the first and second Ag^+ ions were calculated to be 4.46×10^3 and $9.20\times10^4\,M^{-1}$, respectively. The higher K_2 value revealed that a positive allosteric effect participated in the complexation of **L** with the second equivalent of Ag^+. Based on ^1H NMR titration results, we inferred that the two distal bis-enaminone and bis-triazole groups on **L** cooperatively coordinated to Ag^+ ions with the help of cation–π interactions from the phenoxy rings. Furthermore, the ESI-MS spectrometry clearly proved the formation of the homobinuclear complex $\mathbf{L}\cdot(Ag^+)_2$, because a base peak at m/z of 750.1701 was detected and its isotope pattern was in excellent agreement with the calculated one.

Keywords: calixarenes · click chemistry · cycloaddition · fluorescence probes · receptors

Introduction

Over the past few years, the development of fluorescent chemosensors for the selective and sensitive detection of heavy metal ions has attracted considerable attention.[1] Accumulation of heavy metal ions in the bodies of humans and animals can lead to serious illnesses even in low concentration. For example, silver compounds have been widely employed in many industries, such as electronics, photography, and mirrors. Although Ag^+ ions are not essential biologically, its accumulation in the body will influence the activity of enzyme and combine with various metabolites.[2] As a result, the design of selective and sensitive sensors for Ag^+ is of considerable importance for the prevention of environmental pollution and for the protection of human health.[3,4]

Calixarenes, which are the third generation of supramolecules after cyclodextrins and crown ethers, represent very attractive scaffolds for the construction of multivalent binding sites.[5] The rotation of the methylene bridges of calix[4]arene makes its conformation mobile which offers four possible conformational isomers: cone, partial cone, 1,2- and 1,3-alternates.[5a] Among these conformers, the 1,3-alternate conformation, called "smart" conformation of calix[4]arene,[6a] has been proved as a useful scaffold for its versatility on applications, such as nanotubes,[6b–c] dendrimers,[6d–e] and molecular syringes.[6f–g,7a] With symmetrical or unsymmetrical functionalization on both sides of 1,3-alternate calix[4]arene, two binding sites as a potential ditopic ligand are provided, which can accommodate two cations with the help of phenolic oxygen or two π-donor aromatic rings through cation–π interactions (Figure 1).[7]

As part of our continuous interest in the design and synthesis of novel fluorescent chemosensors,[8] we utilized here the 1,3-alternate calix[4]arene platform to construct a ditopic fluorescent sensor, which possessed bis-enaminones and bis-traizoles as two recognition sites and anthracene pendants as fluorophores. Enaminones, also named β-amino-α,β-unsaturated ketones, as one kind of 1,3-bifunctional compounds, have been frequently used as metal ion chelating li-

[a] Dr. I.-T. Ho, K.-C. Haung, Prof. Dr. W.-S. Chung
Department of Applied Chemistry
National Chiao-Tung University
Hsinchu, 30050 (Taiwan)
Fax: (+886) 3-572-3764
E-mail: wschung@nctu.edu.tw

Supporting information for this article is available on the WWW under http://dx.doi.org/10.1002/asia.201100023.

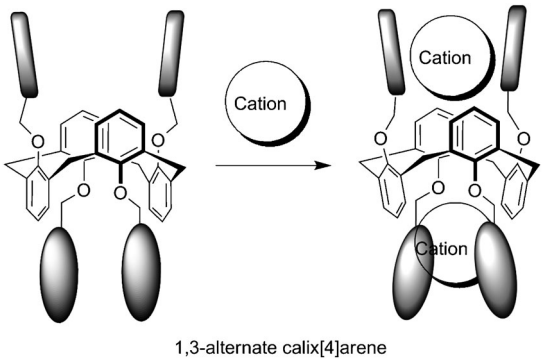

Figure 1. The schematic of 1,3-alternate calix[4]arene as a ditopic receptor for two cations.

gands.[9] Our recent work showed that calix[4]arene with lower-rim distal bis-enaminones can function as a ditopic receptor for the simultaneous complexation of copper and acetate ions.[8a] Furthermore, the advantages of making 1,4-disubstituted-1,2,3-triazoles by click chemistry and their relative stabilities have given rise to many studies in the triazole coordination chemistry.[8b,c,10] For example, recently Yang and Kim independently reported that a pyrenyl-appended triazole substituted calix[4]arene can selectively recognize Zn^{2+} and/or Cd^{2+} ions resulting in ratiometric fluorescent changes of the pyrene monomer and excimer emissions.[10a,g] Moreover, we have demonstrated that a triazole-modified calix[4]crown in 1,3-alternate conformation can behave as a Pb^{2+}/K^{+} off–on switchable fluorescent chemosensor.[8b] Herein, we report the synthesis of 1,3-alternate calix[4]arene **L** and its complexation study with two Ag^{+} ions which shows a six-fold fluorescence quantum yield enhancement. For comparison, the binding ability of the precursor calix[4]arene **4**, which contains the bis-isoxazoles instead of its ring-opened enaminones, was also studied with Ag^{+}.

Results and Discussion

The syntheses of target molecules **4** and **L** are depicted in Scheme 1. The bis-propargyl substituted calix[4]arene **1** reacted with *N*-hydroxybenzimidoyl chloride through 1,3-dipolar cycloaddition to furnish the bis-phenylisoxazole substituted calix[4]arene **2** in 85%.[11] The methylene bridge carbon atoms (Ar*C*H_2Ar) of **2** appeared at 31.2 ppm in its ^{13}C NMR spectrum, which is characteristic of a cone conformation of calix[4]arene (see the Supporting Information, Figure S2).[12] Further alkylation of **2** with propargyl bromide in the presence of Cs_2CO_3 afforded 1,3-alternate dipropargyl calix[4]arene **3** in 41% yield.[13] The 1,3-alternate conformation of **3** was supported by the methylene bridge (Ar*C*H_2Ar) carbon atoms that appeared at 37.5 ppm in the ^{13}C NMR spectrum (see the Supporting Information, Figure S4).[12] Under click chemistry conditions, the 9-(azidomethyl)anthracenes reacted with the two propargyl groups of **3** to form bis-anthrylmethyl-triazole substituted 1,3-alternate

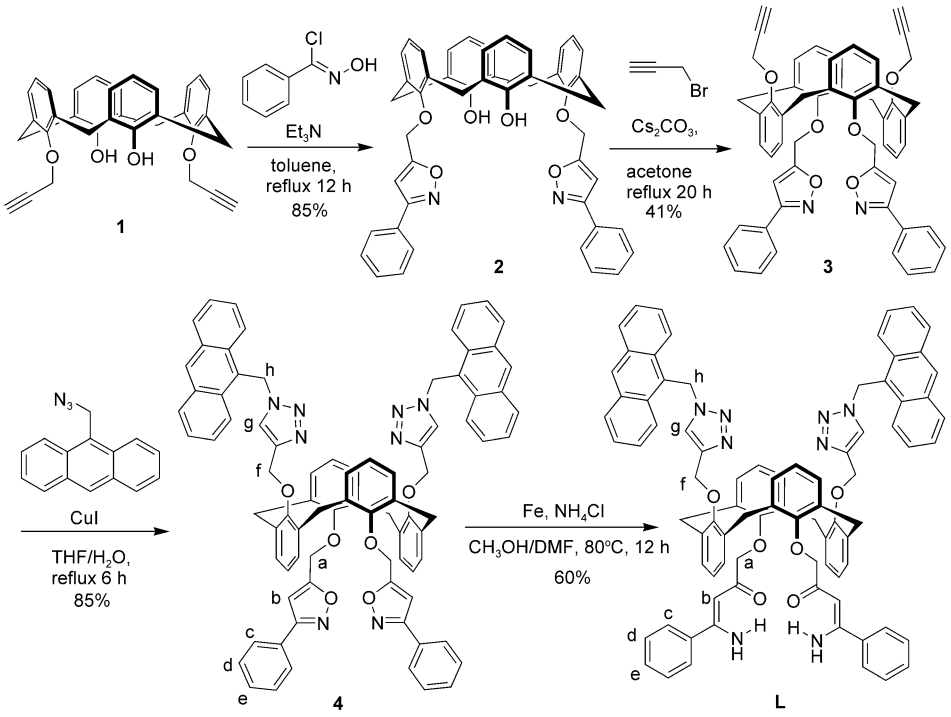

Scheme 1. Syntheses of 1,3-alternate calix[4]arenes **4** and **L**. THF = tetrahydrofuran, DMF = *N*,*N*-dimethylformamide.

Abstract in Chinese:

本文合成設計了一個具有 1,3-交錯構形之芳杯 **L**，其兩端分別修飾上具有蒽基三唑基團與β-胺基-α, β-不飽和酮基團，可作為銀離子的螢光雙位接收器。銀離子與 **L** 錯合時，造成 **L** 的螢光量子產率增強六倍，且在大部分的競爭離子存在時，**L** 維持其對銀離子的選擇性。**L** 對於兩個銀離子的鍵結常數經計算可得 K_1 和 K_2 分別為 4.46×10^3 和 9.20×10^4 M^{-1}。較大的 K_2 表示有一正向的變構效應存在可協助螯合第二個銀離子。氫核磁共振光譜滴定結果顯示，對位雙取代的三唑基團與β-胺基-α, β-不飽和酮基團，在芳杯苯環的 cation-π 作用協助下，分別與銀離子進行螯合。此外，電灑法質譜也明確證實錯合物 **L**·$(Ag^{+})_2$ 的形成，其質譜主要訊號峰 *m*/*z* 750.1701 與經由計算而得的同位素分裂訊號相當吻合。

calix[4]arene **4**, which was evidenced by the appearance of protons H_g of triazoles at 6.23 ppm.[8b] Subsequent N–O bond cleavage of the isoxazole moiety of **4** by Fe powder and NH_4Cl led to corresponding enaminones substituted calix[4]arene **L** in 60% yield.[14] After ring opening reaction of **4**, the proton H_b at 6.02 ppm on the isoxazole ring of **4** was upfield shifted to 5.67 ppm, which was assigned to be the α-unsaturated proton H_b of **L** (see the Supporting Information, Figure S7). In addition, the amino protons were found as two broad signals at 5.51 and 10.31 ppm, in which the most downfield shifted signal was due to the strong intramolecular hydrogen bonding between the amino proton and carbonyl oxygen. All calix[4]arene products **2**, **3**, **4**, and **L** were fully characterized by ^1H and ^{13}C NMR spectroscopy, fast-atom bombardment (FAB) mass spectrometry, and high-resolution mass spectrometry (HRMS; see Experimental Section). The structure and conformation of **L** was further confirmed by a single-crystal X-ray diffraction analysis. The crystal structure of **L** showed a clear saddle-shape of a 1,3-alternate calix[4]arene unit (Figure 2). An interesting feature of the molecular structure of **L** is that one of the anthracene moieties is capping the top of the calix[4]arene cavity through aromatic CH–π interactions,[15] where the nonbonding distances between C10–H and C24–H to the molecular plane of the anthracene ring are 2.29 and 2.69 Å, respectively. Consequently, the other anthracene was pushed away and hung outward, where the triazole ring was orthogonal to the anthracene moiety (Figure 2b). Furthermore, the two enaminone groups were found to orient themselves outward on the lower rim of the 1,3-alternate calix[4]arene **L**.

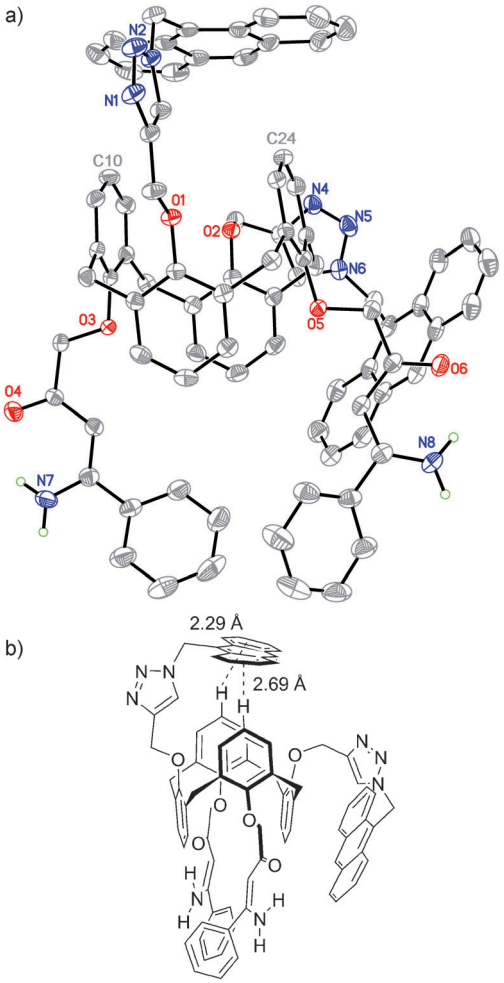

Figure 2. a) X-ray crystallography structure of **L**. All hydrogen atoms are omitted for clarity except the hydrogen atoms on the nitrogen atoms of the enaminone units. b) The side view of structure (a), rotated by 90°.

The selectivity of **L** toward 15 different perchlorate salts of metal ions (Li^+, Na^+, K^+, Mg^{2+}, Ba^{2+}, Ca^{2+}, Cu^{2+}, Hg^{2+}, Cr^{3+}, Pb^{2+}, Ag^+, Mn^{2+}, Zn^{2+}, Cd^{2+}, and Ni^+) in MeOH/$CHCl_3$ (49:1, v/v) was examined by UV/Vis (see the Supporting Information, Figure S9) and fluorescence spectroscopy (Figure 3). As shown in Figure 3, only Ag^+ caused a dramatic fluorescence intensity enhancement of **L** by seven fold. Similar selectivity of Ag^+ by triazole modified chemosensor in MeOH has been previously observed in bis-pyrenyltriazole coupled polyoxyethylenes;[8c] however, in that system, the fluorescence intensity was quenched for Ag^+ binding.

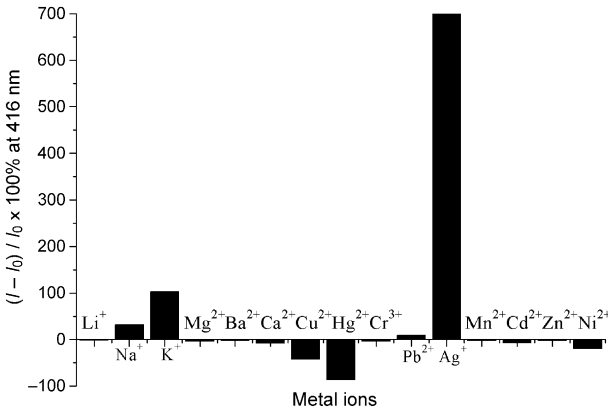

Figure 3. Percentage fluorescence intensity of **L** by the addition of 5 equiv of various metal perchlorates (Li^+, Na^+, K^+, Mg^{2+}, Ca^{2+}, Ba^{2+}, Cr^{3+}, Mn^{2+}, Ni^+, Cu^{2+}, Zn^{2+}, Hg^{2+}, Ag^+, Cd^{2+}, and Pb^{2+}) in MeOH/$CHCl_3$ (49:1, v/v). Excitation wavelength was 370 nm.

To assess the practical applicability of **L** as a Ag^+ selective fluorescent chemosensor, we further carried out the competitive experiments of **L** with Ag^+ in the presence of other metal ions (Li^+, Na^+, K^+, Mg^{2+}, Ca^{2+}, Ba^{2+}, Cu^{2+}, Hg^{2+}, Cr^{3+}, Pb^{2+}, Mn^{2+}, Cd^{2+}, Zn^{2+}, and Ni^{2+}) both at 100 μM. Figure 4 showed that the fluoresce intensity of **L**·$(Ag^+)_2$ was marginally quenched by 30% only upon adding Cu^{2+}, whereas no significant variation was found upon adding all other metal ions. Thus, **L** can be used as a Ag^+ selective fluorescent chemosensor in the presence of most competing cations in cosolvent $CH_3OH/CHCl_3$ (9:1, v/v).

To gain insight into the binding properties of **L** with Ag^+, we further carried out UV/Vis, fluorescence, and ^1H NMR titration studies. The UV/Vis spectrum of **L** exhibits four main absorption bands at 332, 347, 367, and 387 nm, which correspond to the absorptions of enaminone group (λ_{max} =

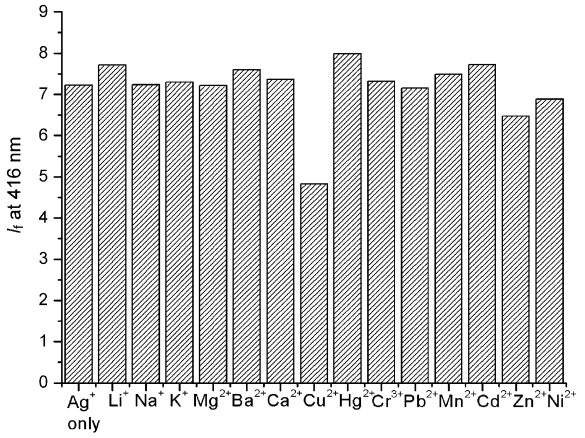

Figure 4. The fluorescence intensity of **L** (20 μM) at 416 nm upon the addition of Ag^+ ions (100 μM) in the presence of other metal ions (100 μM) in MeOH/$CHCl_3$ (49:1, v/v).

332 nm) and anthracene group ($\lambda_{max}=347$, 367, 387 nm), respectively (see the Supporting Information, Figure S10a). On the excitation of **L** at 372 nm, a typical anthracene emission spectrum with a maximum emission band at 416 nm was observed ($\Phi=0.01$, $\Phi_{anthracene}=0.27$ in EtOH as a reference),[16] as shown in Figure 5a. Upon titration with Ag^+, the absorption band at 332 nm gradually increased (see the Supporting Information, Figure S10). Concurrently, the fluorescence intensity of **L** was gradually enhanced by the addition of Ag^+ ions, which gave a fluorescence quantum yield of 0.06 at the saturation level.[16] The Job plot[17] experiment was carried out by using fluorescence intensity as a function of the mole fraction of Ag^+ to determine the binding ratio of **L** with Ag^+. However, the binding ratio could not be obtained because of the irregular variation in the fluorescence changes of **L** with added Ag^+. Furthermore, the curve fitting of the fluorescence titration data of **L** with Ag^+ was unsatisfactory when using Benesi–Hildebrand plot[18] or nonlinear least-squares analysis[19a] assuming a 1:1 complex formation. Thus, a nonlinear least squares analysis for 1:2 ligand-to-metal complexation was considered,[19b] and to our delight the stepwise complexation constants were obtained by excellent fitting of the experimental data to Equation (1):

$$I=\frac{I_0+c_L bK_1[M]+I_{lim}\beta[M]^2}{1+K_1[M]+\beta[M]^2} \quad (1)$$

where $\beta=K_1K_2$ and b is a parameter which includes the molar absorption coefficient (and quantum yield) of the intermediate complex ML. I is the fluorescence intensity of the complex solution. I_o and I_{lim} are the fluorescence intensity for the free ligand **L** and of the complex at saturated level, respectively. c_L and c_M are the total concentration of ligand and metal ion, respectively. [M] is the concentration of the free metal ion. If the approximation $[M]\cong c_M$ is valid, K_1 and β can be determined by a nonlinear least-squares analysis of I versus c_M. As shown in Figure 5b, a satisfactory fitting curve ($R^2=0.9932$) provided two binding constants

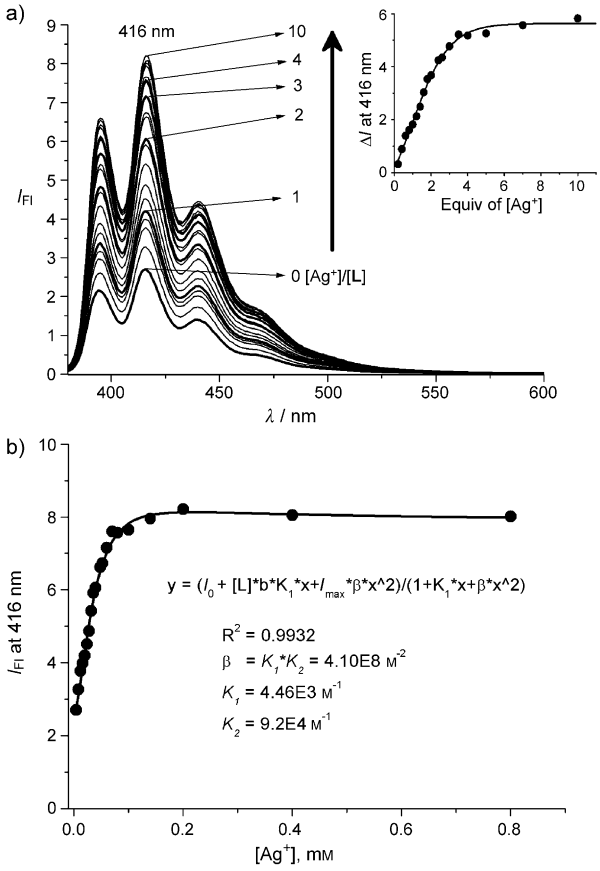

Figure 5. a) The fluorescence emission spectra of **L** (20 μM) with various equivalents of $AgClO_4$ in cosolvent MeOH/$CHCl_3$ (49:1, v/v). Excitation wavelength was 372 nm. The inset shows the variation of fluorescence intensity at 416 nm of **L** by adding different amounts of $AgClO_4$. b) The nonlinear least-squares fitting of **L** with $AgClO_4$.

K_1 and K_2 of **L** with two Ag^+ ions, where $K_1=4.46\times10^3$ and $K_2=9.20\times10^4\,M^{-1}$, respectively. The higher K_2 revealed that a positive allosteric effect[19b,20] participated in the complexation of **L** with the second equivalent of Ag^+. Furthermore, the profiles of the absorbance changes at 332 nm and 387 nm vs. the equivalents of Ag^+ provided the stepwise binding information of **L** with two Ag^+ ions (see the Supporting Information, Figure S10b).[10c,21] Figure S10b showed that the absorbance changes of the triazole linked anthracene at 387 nm were almost saturated by adding 1 equivalent of Ag^+, whereas the absorbance of the enaminone at 332 nm was still increased by adding more than 1 equivalent of Ag^+. The results indicated that the first equivalent of Ag^+ preferred to be bound with the bis-triazole sites and the reoriented structure helped to bind the second equivalent of Ag^+ by the bis-enaminone sites. Notably, the triazoles and enaminones of the single crystal structure of **L** were not preorganized for metal ions binding. Therefore, the conformational reorientation was needed for the stepwise binding of Ag^+ ions, so-called positive allosteric effect.[20]

To gain insight into the possible binding modes of **L** with Ag^+, we further carried out the ^1H NMR titration experi-

ment of **L** with Ag^+. The ^1H NMR spectra of **L** in cosolvent $CD_3OD/CDCl_3$ (9:1, v/v) in the presence of different equivalents of Ag^+ ions are depicted in Figure 6 (for proton labeling on **L,** please see Scheme 1). In the presence of 2 equivalents of Ag^+, the singlet methylene bridge protons at 3.20 ppm were downfield shifted ($\Delta\delta = +1.11$) and split into

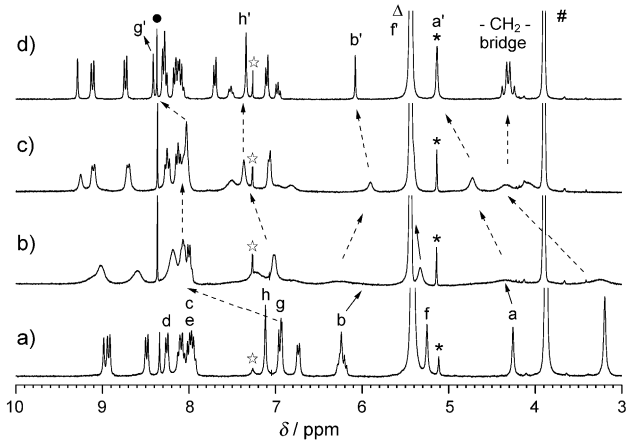

Figure 6. The ^1H NMR titration of **L** (3 mM) in the presence of different amounts of $AgClO_4$ in $CD_3OD/CDCl_3$ (9:1, v/v). a) 0, b) 0.5, c) 1.0 and d) 2.0. #: CHD_2OD, *: CD_3OH, △: H_2O, ☆: external $CHCl_3$, ●: internal $CHCl_3$.

an AB quartet (4.28 and 4.35 ppm, $J = 15.8$ Hz), which implied that the phenoxy rings of 1,3-altenate calix[4]arene were distorted. The enaminone units also exhibited substantial changes when complexed with Ag^+, where the nearby methylene protons (H_a) were downfield shifted from 4.25 to 5.13 ppm ($\Delta\delta = +0.88$) and the methine protons (H_b) around 6.20–6.35 ppm (overlapped with aromatic signals of calix[4]-arene) were upfield shifted ($\Delta\delta = -0.16$). Furthermore, the methylene protons (H_f, 5.25 ppm) linking the triazole units to the calix[4]arene skeleton were downfield shifted by 0.2 ppm and the triazole methine proton (H_g) was most downfield shifted ($\Delta\delta = +1.47$) among all protons. All the proton signals of **L** were broadened by adding 0.5 to 1 equivalent of Ag^+, which became sharp again after adding 2 equivalents of Ag^+. Such a peak broadening at 1 equivalent of Ag^+ may be attributed to the faster rate of the complexation–decomplexation than the NMR time scale at 25 °C.[7a] The second equivalent of Ag^+ was bound by **L**·Ag^+ through a cooperative binding effect of the first Ag^+ ion, thus resulted in the formation of a more stable complex **L**·$(Ag^+)_2$, which showed sharp signals again (Figure 6 d).Variable temperature (−50 to 50 °C) ^1H NMR spectroscopy of **L** with 1 equivalent of Ag^+ was also carried out, which exhibited sharp peaks at −50 °C due to the slower rate of the complexation–decomplexation processes at low temperature (see the Supporting Information, Figure S13). In principle, a bound Ag^+ may tunnel through the π-basic tube of 1,3-alternate calix[4]arene to another binding site; however, it was not observed in **L**·Ag^+ even at 50 °C.[6e,f] Based on these observations, we suggested that the two Ag^+ ions were tightly bound within the two cavities, which consisted of the bis-enaminone units and the bis-triazole groups on the 1,3-alternate calix[4]arene **L**. Furthermore, the π-rich phenoxy rings on calix[4]arene were supposed to participate in the complexation through a cation–π interaction, as has been reported in other ditopic calix[4]thiacrowns for the complexation of Ag^+ ions.[4c,7a,22]

The ESI-MS spectrum of the complex **L**·$(Ag^+)_2$ provided further evidence for the 1:2 ligand–metal complexation, as shown in Figure 7 (full spectrum is shown in the Supporting Information, Figure S14). Comparison of the measured isotope pattern with the calculated one supported the composi-

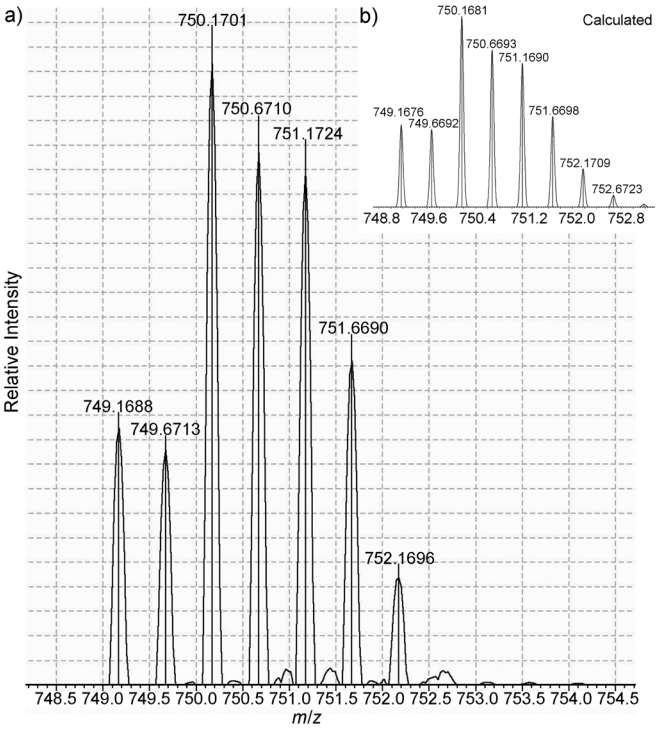

Figure 7. The ESI-MS spectrum of the complex **L**·$(Ag^+)_2$, where the inset is the calculated MS spectrum for the complex **L**·$(Ag^+)_2$ (formula: $[C_{84}H_{68}N_8O_6Ag_2]^{2+}$).

tion of the base peak at m/z 750.1701 to be the complex **L**·$(Ag^+)_2$ ($[C_{84}H_{68}N_8O_6Ag_2]^{2+}$). Note that no deprotonation during complexation was observed based on the ESI-MS data.

To further elucidate the binding modes of **L** with 2 equivalents of Ag^+, we also investigated the binding affinity of precursor **4** toward Ag^+ by fluorescence titration experiment (Figure 8). The isoxazole substituted calix[4]arene **4** exhibited a higher fluorescence quantum yield ($\Phi = 0.18$)[16] compared to the enaminone substituted **L** ($\Phi = 0.01$), suggesting that the bis-enaminone moieties are more flexible than the bis-isoxazole groups, and are therefore more prone to radiationless decay. In contrast to **L**, the fluorescence intensity of **4** was gradually decreased upon adding various amounts of Ag^+ ($\Phi = 0.08$)[16] and the intensity changes

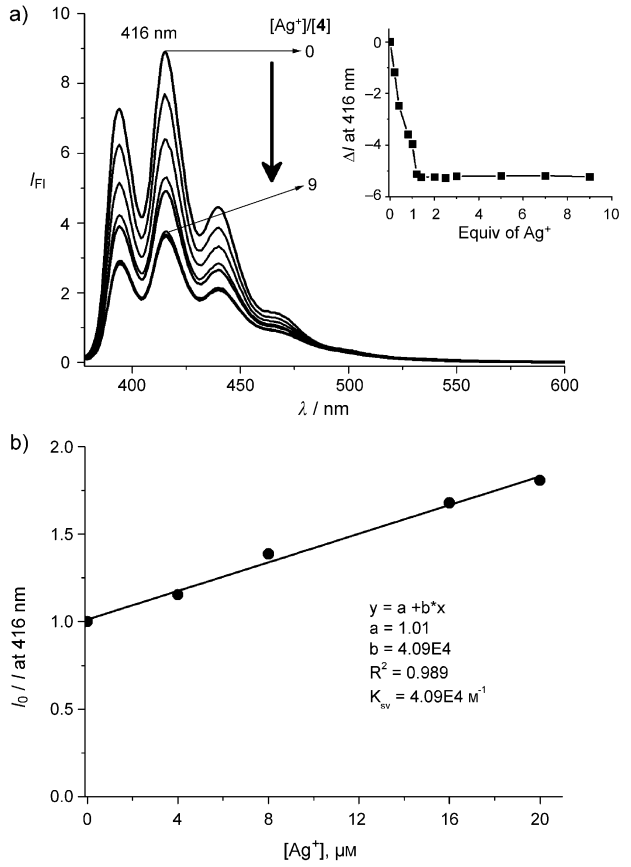

Figure 8. a) The fluorescence emission spectra of **4** (20 μM) with various equivalents of $AgClO_4$ in $MeOH/CHCl_3$ (49:1, v/v). Excitation wavelength was 372 nm. The inset shows the variation in fluorescence intensity at 416 nm of **4** by adding different amounts of $AgClO_4$. b) The Stern–Volmer plot of **4** with $AgClO_4$.

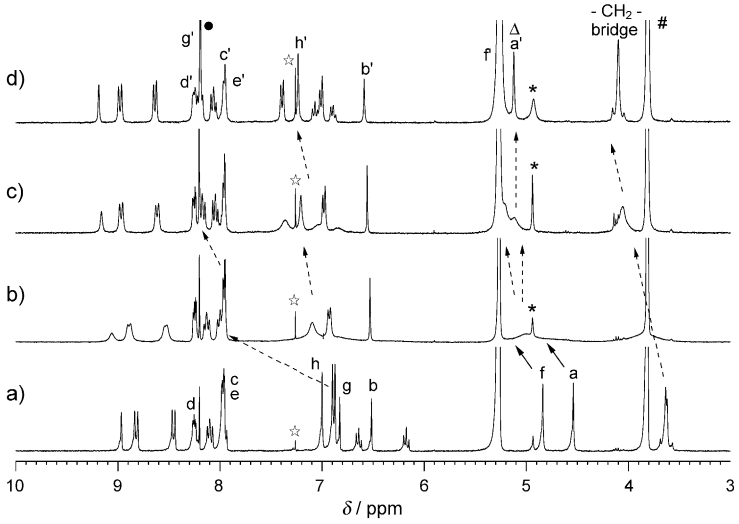

Figure 9. The ^1H NMR titration spectra of **4** (3 mM) in the presence of different amounts of $AgClO_4$ in $CD_3OD/CDCl_3$ (3:1, v/v). a) 0, b) 0.5, c) 1.0, and d) 1.5. #: CHD_2OD, *: CD_3OH, △: H_2O, ☆: external $CHCl_3$, ●: internal $CHCl_3$.

were saturated at 1 equivalent of Ag^+ ion. The Job plot measurement was also carried out between **4** and Ag^+ (see the Supporting Information, Figure S18b),[17] where the fluorescence intensity changes at 416 nm reached a maximum at a mole fraction of 0.5 of **4** indicating the 1:1 binding ratio between **4** and Ag^+. Moreover, the binding constant was calculated to be $4.09\times10^4\,M^{-1}$ by the Stern–Volmer plot (Figure 8b).[23]

The ^1H NMR titration spectra of **4** with various equivalents of Ag^+ in cosolvent $CD_3OD/CDCl_3$ (3:1, v/v) are shown in Figure 9 (for proton labeling of **4**, please see Scheme 1). The methylene bridge protons of **4** were downfield shifted by 0.47 ppm, which was smaller compared to that of **L**. In addition, the methylene protons (H_f, 4.84 ppm) near the triazoles and the triazole protons (H_g, 6.83 ppm) were both significantly downfield shifted by ca. 0.41 and 1.36 ppm, respectively. Such downfield shifts of H_f and H_g in the metal complex of **4** indicated that Ag^+ was chelated by the nitrogen atoms of the bis-triazole groups. By contrast, the methine protons (H_b, 6.52 ppm) on the isoxazole ring of **4** were almost unchanged by the addition of Ag^+, which implied that the isoxazole groups did not participate in the complexation with Ag^+. Although the methylene protons (H_a, 4.54 ppm) near the isoxazoles of **4** were downfield shifted by 0.38 ppm, it was regarded as the result of the conformational change due to the complexation of Ag^+ by the bis-triazole groups. The structure of the metal complex, **4**·Ag^+, was further supported by the ESI-MS spectrum (Figure 10), which displayed an excellent correlation with the calculated isotope pattern of **4**·Ag^+ ($[C_{84}H_{64}N_8O_6Ag]^+$) at its base

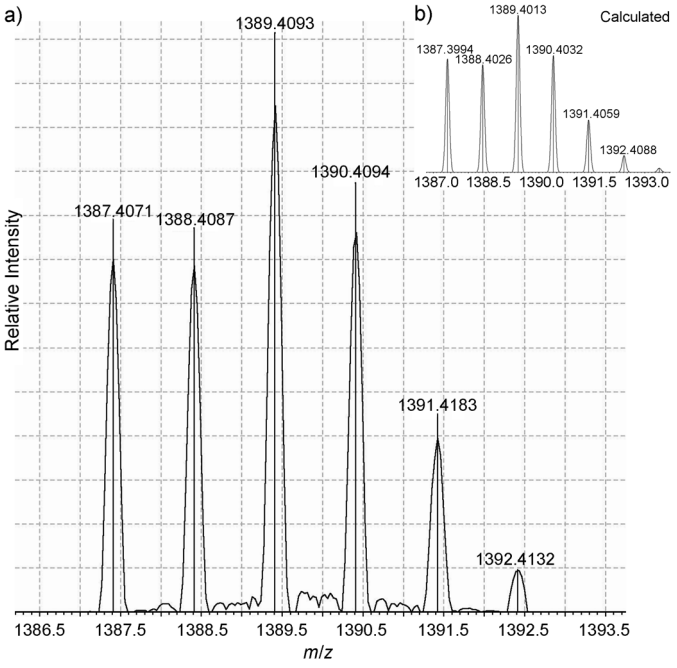

Figure 10. The ESI-MS spectrum of the complex **4**·Ag^+, where the inset is a calculated spectrum for the complex **4**·Ag^+ (formula: $[C_{84}H_{64}N_8O_6Ag]^+$).

peak *m*/*z* 1389.4039 (full spectrum is shown in the Supporting Information, Figure S15).

Based on all these results, possible binding modes of the complexes **4**·Ag^+ and **L**·$(Ag^+)_2$ are proposed and depicted in Scheme 2. The two triazole rings of **4** participated in the complexation with Ag^+ resulted in the fluorescence quenching of the nearby anthracenes, which was presumably owing

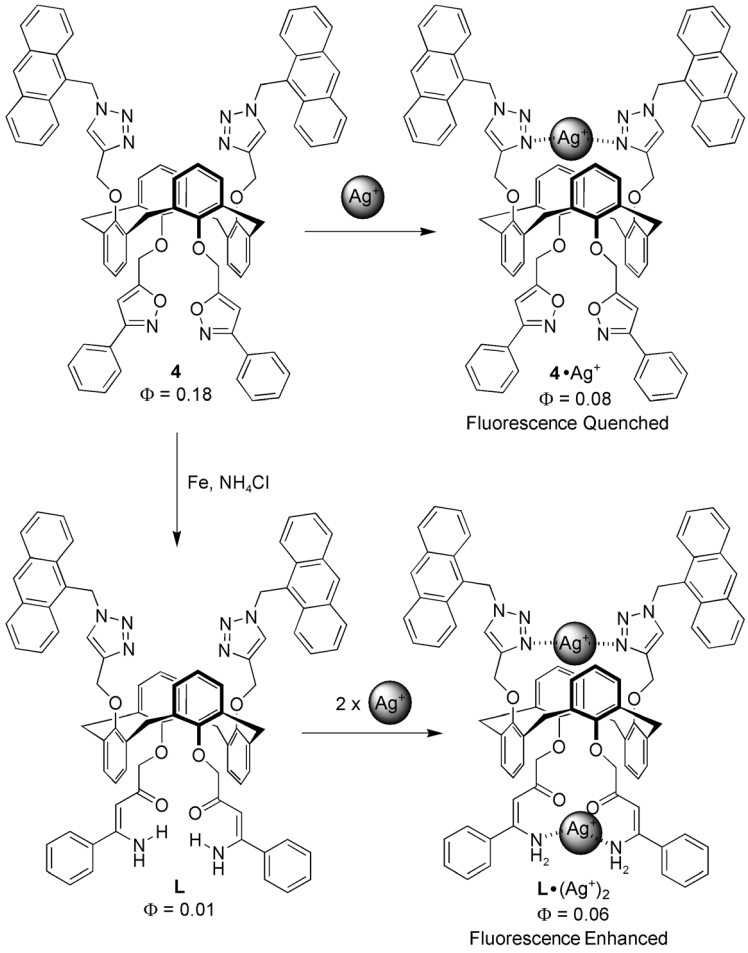

Scheme 2. Possible binding modes of **4** and **L** with Ag^+ ion(s).

to the inverse photoinduced electron transfer (PET)[24] from anthracenes to the Ag^+-bound nitrogen atoms in the triazole rings, the electron density of which might have been decreased by metal ion complexation. The target ligand **L**, which was obtained after the ring-opening reaction of bis-isoxazolyl phenyl of **4**, exhibited a weaker emission quantum yield ($\Phi = 0.01$) due to the flexibility of the enaminone groups. When two Ag^+ ions were complexed by **L**, one was chelated by the two distal enaminones and the other by the two distal triazoles, and both complexations were also assisted by cation–π interactions through the phenoxy rings. The fluorescence intensity of **L**·$(Ag^+)_2$ was enhanced compared to that of the free host **L**, which was mainly due to the conformational restriction of the two enaminone groups when they chelated with Ag^+. Although the inverse PET from anthracene to the nitrogen atoms of the triazole rings of **L**·$(Ag^+)_2$ was expected to decrease the fluorescence quantum yield, nevertheless, it turned out to be a minor factor in affecting the overall fluorescence intensity.

Conclusions

In summary, we have synthesized a novel 1,3-alternate calix[4]arene **L** with bis-triazoles and bis-enaminones on each end, which acted as a homobinuclear ditopic fluorescent chemosensor for Ag^+ ions. The binding of Ag^+ by **L** resulted in a strong fluorescence enhancement due to complexation-induced rigidity of its structure. In the presence of most competing metal ions, **L** retained its selectivity toward Ag^+ ion. On the other hand, precursor **4** without the ring-opening enaminone moieties lost the ability to recognize two Ag^+ ions simultaneously. Moreover, the complexation of **4** with Ag^+ led to a severe fluorescence quenching due to an inverse PET from anthracenes to the Ag^+ bound nitrogen atoms of the triazole rings. Hence, by the judicious design and synthesis of chelation ligands on both sides of the 1,3-alternate calix[4]arene skeleton using click chemistry, 1,3-dipolar cycloaddition, and subsequent ring-opening protocol, one can selectively bind one or 2 equivalents of Ag^+ ions with opposite fluorescence responses. Work toward developing other useful chromogenic and fluorogenic ligands using this protocol and click chemistry is in progress in our group.

Experimental Section

^{1}H NMR spectra were measured on either a 300 or 500 MHz spectrometer. Natural abundance ^{13}C NMR spectra were measured using pulse Fourier transform, on a 300 or a 500 MHz NMR spectrometer operating at 75.4 and 125.7 MHz. Broad-band decoupling, distortionless enhancement by polarization transfer (DEPT), heteronuclear multiple quantum coherence (HMQC), and heteronuclear multiple bond coherence (HMBC) were carried out to simplify spectra and aid peak identification. All reported yields were from an average of three runs and were based on uncovered starting materials.

2: To a well-stirred solution of 25,27-dipropargyloxy-26,28-dihydroxycalix[4]arene **1** (1.40 g, 2.80 mmol) and *N*-hydroxybenzimidoyl chloride (1.31 g, 8.40 mmol) in THF (50 mL), excess triethylamine (1.16 mL, 8.40 mmol) was slowly added. The reaction mixture was stirred at reflux for 12 h, diluted with dichloromethane, washed with water, and dried over $MgSO_4$. After filtration and evaporation of the solvent, the residue was recrystallized by CH_2Cl_2/MeOH (120mL, v/v = 5:1) which gave the cycloadduct **2** in 85% yield. Pale-yellow solid; m.p. 254–256 °C; $R_f = 0.36$ (hexane/EtOAc = 5:1); ^{1}H NMR ($CDCl_3$, 300 MHz): $\delta_H = 3.38$ (d, $J = 13.3$ Hz, 4H; ArCH_2Ar), 4.26 (d, $J = 13.3$ Hz, 4H; ArCH_2Ar), 5.24 (s, 4H; OCH_2), 6.68–6.76 (m, 4H, aromatic), 6.87 (d, $J = 7.5$ Hz, 4H; aromatic), 6.90 (s, 2H; C*H* of isoxazole), 7.08 (d, $J = 7.5$ Hz, 4H; aromatic), 7.24 (s, 2H; O*H*), 7.40–7.43 (m, 6H; Ph-*H*), 7.75–7.78 ppm (m, 4H; Ph-*H*); ^{13}C NMR ($CDCl_3$, 75.4 MHz): $\delta_c = 31.2$ (CH_2), 68.4 (CH_2), 102.2 (CH), 119.4 (CH), 126.0 (CH), 126.8 (CH), 127.8 (C_q), 128.5 (C_q), 128.6 (CH), 128. (CH), 129.2 (CH), 130.1 (CH), 132.9 (C_q), 151.4 (C_q), 152.9 (C_q), 162.5 (C_q), 167.7 ppm (C_q). MS (FAB, *m*/*z*) 739 [*M*+H$^+$]; HRMS *m*/*z* calcd. for $C_{48}H_{39}N_2O_6$ 739.2808; found 739.2811.

3: To a stirred suspension of compound **2** (1.20 g, 1.62 mmol) and Cs_2CO_3 (5.28 g, 16.2 mmol) in 200 mL acetone was added propargyl bromide (1.44 mL, 16.2 mmol); the reaction mixture was stirred under reflux for 5 h. The solvent was removed under reduced pressure and the residue was treated with CH_2Cl_2 (20 mL) and water (50 mL). The organic phase was washed twice with water (2×50 mL), dried over $MgSO_4$, and the solvent was evaporated. TLC analysis of the residue showed the presence of three isomers (1,3-*alt*, *cone* and *paco*). Column chromatography on silica gel eluting with hexane and ethyl acetate gave the white solid compounds **3** in 41% yield. White solid; m.p. 173–174°C; R_f=0.21 (hexane/EtOAc=5:1); ^{1}H NMR ($CDCl_3$, 300 MHz): δ_H=2.40 (t, J=2.4 Hz, 2H; CC*H*), 3.63 (d, J=15.3 Hz, 4H; ArCH_2Ar), 3.90 (d, J=15.3 Hz, 4H; ArCH_2Ar), 4.00 (d, J=2.4 Hz, 4H; OCH_2CCH), 4.49 (s, 4H; OCH_2), 6.10 (s, 2H; C*H* of isoxazole), 6.59 (t, J=7.5 Hz, 2H; aromatic), 6.88–6.93 (m, 6H; aromatic), 7.20 (d, J=7.5 Hz, 4H; aromatic), 7.44–7.50 (m, 6H; Ph-*H*), 7.81–7.84 ppm (m, 4H; Ph-*H*); ^{13}C NMR ($CDCl_3$, 75.4 MHz): δ_c=37.5-(CH_2), 58.5 (CH_2), 63.8 (CH_2), 74.7 (CH_3), 80.2 (CH_3), 101.7 (CH), 123.2 (CH), 123.7 (CH), 126.8 (CH), 128.9 (CH), 129.0 (CH), 130.0 (CH), 130.1 (CH), 130.6 (CH), 134.1 (C_q), 134.5 (C_q), 155.1 (C_q), 155.3 (C_q), 162.2 (C_q), 169.1 ppm (C_q). MS (FAB, *m*/*z*) 815 [*M*+H$^+$]; HRMS *m*/*z* calcd for $C_{54}H_{42}N_2O_6$ 815.3121; found 815.3113.

4: To a well-stirred solution of compound **3** (410 mg, 0.50 mmol) and 9-(azidomethyl)anthracene (246 mg, 1.05 mmol) in THF/H_2O (70 mL, v/v=6:1) was added CuI (65 mg, 0.25 mmol). The reaction mixture was stirred under reflux for 6 h. After evaporation of the solvent, the residue was dissolved in CH_2Cl_2 and extracted with H_2O. The organic layer was dried over $MgSO_4$ and the filtrate was concentrated under reduced pressure. The solid product was purified by column chromatography to afford pure compound **4** in 72% yield. Pale-yellow solid; m.p. 129–132°C; R_f=0.15 (hexane/EtOAc=2:1); ^{1}H NMR ($CDCl_3$, 300 MHz): δ_H=3.11 (s, 8H; ArCH_2Ar), 4.03 (s, 4H; H_a), 4.43 (s, 4H; H_f), 5.57 (t, J=7.4 Hz, 2H; aromatic), 6.02 (s, 2H; H_b), 6.16 (t, J=7.4 Hz, 2H; aromatic), 6.23 (s, 2H; H_g), 6.36–6.43 (m, 8H; aromatic), 6.46 (s, 4H; H_h), 7.45–7.51 (m, 10H; Ph-*H* and Anthracene-*H*), 7.58–7.63 (m, 4H; Anthracene-*H*), 7.78–7.81 (m, 4H; Ph-*H*), 8.00 (d, J=8.4 Hz, 4H; Anthracene-*H*), 8.27 (d, J=8.9 Hz, 4H; Anthracene-*H*), 8.51 ppm (s, 2H; Anthracene-*H*); ^{13}C NMR ($CDCl_3$, 75.4 MHz): δ_c=36.8(CH_2), 46.2 (CH_2), 63.7 (CH_2), 63.8 (CH_2), 101.2 (CH), 122.0 (CH), 122.4 (CH), 122.6 (CH), 122.9 (CH), 123.8 (C_q), 125.4 (CH), 126.7 (CH), 127.6 (CH), 129.0 (CH), 129.8 (CH), 130.0 (CH), 130.3 (CH), 130.6 (C_q), 131.4 (C_q), 133.4 (C_q), 134.2 (C_q), 144.0 (C_q), 154.5 (C_q), 154.7 (C_q), 162.0 (C_q), 169.3 ppm (C_q); MS (FAB, *m*/*z*) 1282 [*M*+H$^+$]; HRMS *m*/*z* calcd for $C_{84}H_{64}N_8O_6$ 1281.5027; found 1281.5011.

L: To a stirred solution of compound **4** (140 mg, 0.11 mmol) and NH_4Cl (60 mg, 1.10 mmol) in DMF and MeOH (1:1, 6 mL) was added Fe powder (60 mg, 1.10 mmol). The reaction mixture was heated to 80°C and was allowed to stir at this temperature for 12 h. The mixture was cooled to room temperature, diluted with CH_2Cl_2, and filtered out through a silica gel covered celite pad. The filtrate was washed by diluted HCl and H_2O, dried over $MgSO_4$, and evaporated under vacuum. The residue was then purified by column chromatography to afford pure **L** in 60% yield. Single crystals of **L** for X-ray crystallography were prepared by slow diffusion of hexane into the chloroform solution of **L**. Yellow solid; m.p. 204–206°C; R_f=0.15 (hexane/EtOAc=1:4); ^{1}H NMR ($CDCl_3$, 300 MHz): δ_H=2.92 and 3.02 (ABq, J=13.7 Hz, 8H; ArCH_2Ar), 3.94 (s, 4H; H_a), 4.71 (s, 4H; H_f), 5.31 (t, J=7.5 Hz, 2H; aromatic), 5.51 (bs, 2H; NH_2), 5.67 (s, 2H; H_b), 5.91 (t, J=7.5 Hz, 2H; aromatic), 6.36 (d, J=7.5 Hz, 4H; aromatic), 6.50 (d, J=7.5 Hz, 4H; aromatic), 6.50 (s, 2H; H_g), 6.54 (s, 4H; H_h), 7.36–7.61 (m, 18H; Ph-*H* and Anthracene-*H*), 8.02 (d, J=8.3 Hz, 4H; Anthracene-*H*), 8.32 (d, J=8.9 Hz, 4H; Anthracene-*H*), 8.53 (s, 2H; Anthracene-*H*), 10.31 ppm (bs, 2H; NH_2); ^{13}C NMR ($CDCl_3$, 75.4 MHz): δ_c=35.4 (CH_2), 46.2 (CH_2), 64.8 (CH_2), 76.1 (CH_2), 92.1 (CH), 120.8 (CH), 121.7 (CH), 122.7 (CH), 122.9 (CH), 124.0 (C_q), 125.4 (CH), 126.3 (CH), 127.7 (CH), 129.0 (CH), 129.5 (CH), 129.8 (CH), 129.9 (CH), 130.4 (CH), 130.7 (C_q), 131 (CH), 131.5 (C_q), 132.4 (C_q), 133.7 (C_q), 136.4 (C_q), 144.5 (C_q), 154.3 (C_q), 154.9 (C_q), 161.7 (C_q), 195.1 ppm (C_q); MS (FAB, *m*/*z*)1286 [*M*+H$^+$]; HRMS *m*/*z* calcd for $C_{84}H_{69}N_8O_6$ 1285.5340; found 1285.5331.

X-ray crystal data for **L**: $C_{87}H_{71}Cl_9N_8O_6$, M=1643.57, monoclinic, a=21.0890(5) Å, b=16.6481(4) Å, c=22.5350(9) Å, α=90°, β=96.398(3)°, γ=90°, V=4559.4(4) Å^3, space group $P2_1/n$, Z=4, calculated density 1.388 Mg m^{-3}, crystal dimensions (mm^3): 0.25×0.20×0.15, T=150(2) K, λ ($Mo_{K\alpha}$)=1.54178 Å, μ=3.421 mm^{-1}, 23873 reflections collected, 14150 independent (R_{int}=0.0278), 991 parameter refined on F^2, R_1=0.0704, $wR2[F^2]$=0.1797 (all data), goodness-of-fit (GOF) on F^2 1.285, $\Delta\rho_{max}$=1.452 e Å^{-3}. CCDC 806595 contains the supplementary crystallographic data for this paper. These data can be obtained free of charge from the Cambridge Crystallographic Data Centre via www.ccdc.cam.ac.uk/data_request/cif.

General Procedure for the UV/Vis and Fluorescence Experiments

UV/Vis spectra were recorded with a HP-8453 spectrophotometer equipped with a diode array detector, and the resolution was set at 1 nm. Fluorescence spectra were recorded with an Aminoco Bowman Series-2-type spectrofluorometer. For all measurements of fluorescence spectra, excitation was at 308 nm with the excitation and emission slit width at 4.0 nm. UV/Vis and fluorescence titration experiments were performed with 20 μM solutions of **L** and **4** and varying concentrations of metal perchlorate in MeOH/$CHCl_3$ (49:1, v/v). During the measurements, the temperature of the quartz sample cell and chamber was kept at 25°C.

General Procedure for the ^{1}H NMR Titration Experiments

^{1}H NMR titration spectra were recorded at 300 MHz with tetramethylsilane (TMS) in a coaxial capillary tube as an external standard. Experiments were performed with 3 mM solutions of **L** and **4** in $CD_3OD/CDCl_3$ (9:1 and 3:1 v/v, respectively) by adding various concentrations of $AgClO_4$ at 25°C.

Acknowledgements

We thank the National Science Council (NSC) and the MOE ATU program of the Ministry of Education, Taiwan, the Republic of China, for financial support.

[1] a) A. P. de Silva, H. Q. N. Gunaratne, T. Gunnlaugsson, A. J. M. Huxley, C. P. McCoy, J. T. Rademacher, T. E. Rice, *Chem. Rev.* **1997**, *97*, 1515–1566; b) J.-P. Desvergne, A. W. Czarnik in *Chemosensors of Ion and Molecular Recognition*, Kluwer, Dordrecht, **1997**; c) B. Valeur, I. Leray, *Coord. Chem. Rev.* **2000**, *205*, 3–40; d) L. Prodi, F. Bolletta, M. Montalti, N. Zaccheroni, *Coord. Chem. Rev.* **2000**, *205*, 59–83.

[2] a) H. T. Ratte, *Environ. Toxicol. Chem.* **1999**, *18*, 89–108; b) M. R. Ganjali, P. Norouzi, T. Alizadeh, M. Adib, *J. Braz. Chem. Soc.* **2006**, *17*, 1217–1222; c) X. B. Zhang, Z. X. Han, Z. H. Fang, G. L. Shen, R. Q. Yu, *Anal. Chim. Acta* **2006**, *562*, 210–215.

[3] a) L. Liu, D. Zhang, G. Zhang, J. Xiang, D. Zhu, *Org. Lett.* **2008**, *10*, 2271–2274; b) X. Zhu, S. Fu, W.-K. Wong, W.-Y. Wong, *Tetrahedron Lett.* **2008**, *49*, 1843–1846; c) K. M. K. Swamy, H. N. Kim, J. H. Soh, Y. Kim, S.-J. Kim, J. Yoon, *Chem. Commun.* **2009**, 1234–1234; d) L. Liu, G. Zhang, J. Xiang, D. Zhang, D. Zhu, *Org. Lett.* **2008**, *10*, 4581–4584; e) Z. Xu, S. Zheng, J. Yoon, D. R. Spring, *Analyst* **2010**, *135*, 2554–2559; f) C. Zhao, K. Qu, Y. Song, C. Xu, J. Ren, X. Qu, *Chem. Eur. J.* **2010**, *16*, 8147–8154.

[4] For calix[4]arenes-based chemosensors toward Ag^+, see: a) R. Joseph, B. Ramanujam, A. Acharya, C. P. Rao, *J. Org. Chem.* **2009**, *74*, 8181–8190; b) J. S. Kim, O. J. Shon, J. A. Rim, S. K. Kim, J. Yoon, *J. Org. Chem.* **2002**, *67*, 2348–2351; c) J. Y. Lee, J. Kwon, C. S. Park, J.-E. Lee, W. Sim, J. S. Kim, J. Seo, I. Yoon, J. H. Jung, S. S. Lee, *Org. Lett.* **2007**, *9*, 493–496; d) T. Yamato, C. Perez-Casas, A. Yoshizawa, S. Rahman, M. R. J. Elsegood, C. Redshaw, *J. Inclusion Phenom. Macrocyclic Chem.* **2009**, *63*, 301–308; e) B. S. Creaven, M. Deasy, P. M. Flood, J. McGinley, B. A. Murray, *Inorg. Chem. Commun.* **2008**, *11*, 1215–1220.

[5] a) C. D. Gutsche in *Calixarenes Monographs in Supramolecular Chemistry*, *Vol. 1* (Ed.: J. F. Stoddart), The Royal Society of Chemistry, Cambridge, **1989**, pp. 127–148; b) C. D. Gutsche in *Calixarenes Revisited Monographs in Supramolecular Chemistry*, *Vol. 6* (Ed.: J. F. Stoddart), The Royal Society of Chemistry: Cambridge, **1998**, pp. 79–145; c) A. Ikeda, S. Shinkai, *Chem. Rev.* **1997**, *97*, 1713–1734; d) L. Baldini, A. Casnati, F. Sansone, R. Ungaro, *Chem. Soc. Rev.* **2007**, *36*, 254–266.

[6] a) L. Baklouti, J. Harrowfield, B. Pulpoka, J. Vicens, *Org. Chem.* **2006**, *3*, 355–384, and references therein; b) G. V. Zyryanov, D. M. Rudekevich, *J. Am. Chem. Soc.* **2004**, *126*, 4264–4270; c) V. G. Organo, A. V. Leontiev, V. Sgarlata, H. V. R. Dias, D. M. Rudekevich, *Angew. Chem.* **2005**, *117*, 3103–3107; *Angew. Chem. Int. Ed.* **2005**, *44*, 3043–3047; d) Y. Rudzevich, K. Fischer, M. Schmidt, V. Böhmer, *Org. Biomol. Chem.* **2005**, *3*, 3916–3925; e) V. Štastný, I. Stibor, H. Dvořáková, P. Lhoták, *Tetrahedron* **2004**, *60*, 3383–3391; f) A. Ikeda, T. Tsudera, S. Shinkai, *J. Org. Chem.* **1997**, *62*, 3568–3574; g) J. S. Kim, S. H. Yang, J. A. R. , J. Y. Kim, J. Vicens, S. Shinkai, *Tetrahedron Lett.* **2001**, *42*, 8047–8050.

[7] a) A. Ikeda, S. Shinkai, *J. Am. Chem. Soc.* **1994**, *116*, 3102–3110; b) R. Ungaro, A. Casnati, F. Ugozzoli, A. Pochini, J.-F. Dozol, C. Hill, H. Rouquette, *Angew. Chem.* **1994**, *106*, 1551–1553; *Angew. Chem. Int. Ed. Engl.* **1994**, *33*, 1506–1509; c) S. Kim, J. S. Kim, S. K. Kim, I.-H. Suh, S. O. Kang, J. Ko, *Inorg. Chem.* **2005**, *44*, 1846–1851; d) J. S. Kim, H. J. Kim, H. M. Kim, S. H. Kim, J. W. Lee, S. K. Kim, B. R. Cho, *J. Org. Chem.* **2006**, *71*, 8016–8022.

[8] a) A. Senthilvelan, I-T. Ho, K.-C. Chang, G.-H. Lee, Y.-H. Liu, W.-S. Chung, *Chem. Eur. J.* **2009**, *15*, 6152–6160; b) K.-C. Chang, I.-H. Suo, A. Senthilvelan, W.-S. Chung, *Org. Lett.* **2007**, *9*, 3363–3366; c) H.-C. Hung, C.-W. Cheng, Y.-Y. Wang, Y.-J. Chen, W.-S. Chung, *Eur. J. Org. Chem.* **2009**, 6360–6366.

[9] For enaminone compounds as chelation units, please see: a) J. R. Bradbury, J. L. Hampton, D. P. Martone, A. W. Maverick, *Inorg. Chem.* **1989**, *28*, 2392–2399; b) A. W. Maverick, F. R. Fronczek, D. P. Martone, *J. Coord. Chem.* **1989**, *20*, 149–161; c) D. Jones, A. Roberts, K. Cavell, W. Keim, U. Englert, B. W. Skelton, A. H. White, *J. Chem. Soc. Dalton Trans.* **1998**, 255–262; d) U. Pietrasik, J. Szydlowska, A. Krówczyński, D. Pociecha, E. Górecka, D. Guillon, *J. Am. Chem. Soc.* **2002**, *124*, 8884–8890; e) G. W. Everett, Jr., R. H. Holm, *J. Am. Chem. Soc.* **1965**, *87*, 2117–2127; f) Jr. H. F. Holtzclaw, J. P. Collman, R. M. Alire, *J. Am. Chem. Soc.* **1958**, *80*, 1100–1103.

[10] a) S. Y. Park, J. H. Yoon, C. S. Hong, R. Souane, J. S. Kim, S. E. Mathews, J. Vicens, *J. Org. Chem.* **2008**, *73*, 8212–8218; b) J. Zhan, D. Tian, H. Li, *New J. Chem.* **2009**, *33*, 725–728; c) B. Colasson, M. Save, P. Milko, J. Roithova, D. Schröder, O. Reinaud, *Org. Lett.* **2007**, *9*, 4987–4990; d) G. F. Manbeck, W. W. Brennessel, C. M. Evans, R. Eisenberg, *Inorg. Chem.* **2010**, *49*, 2834–2843; e) S. H. Kim, H. S. Choi, J. Kim, S. J. Lee, D. T. Quang, J. S. Kim, *Org. Lett.* **2010**, *12*, 560–563; f) M. L. Gower, J. D. Crowley, *Dalton Trans.* **2010**, *39*, 2371–2378; g) L.-N. Zhu, S.-L. Gong, S.-L. Gong, C.-L. Yang, J.-G. Qin, *Chin. J. Chem.* **2008**, *26*, 1424–1430.

[11] a) C.-M. Shu, G.-H. Lee, S.-M. Peng, W.-S. Chung, *J. Chin. Chem. Soc.* **2000**, *47*, 173–182; b) Y.-J. Shiao, P.-C. Chiang, A. Senthilvelan, M.-T. Tsai, G.-H. Lee, W.-S. Chung, *Tetrahedron Lett.* **2006**, *47*, 8383–8386.

[12] C. Jaime, J. de Mendoza, P. Prados, P. M. Nieto, C. Sánchez, *J. Org. Chem.* **1991**, *56*, 3372–3376.

[13] a) M. J. Chetcuti, A. M. J. Devoille, A. B. Othman, R. Souane, P. Thuéry, J. Vicens, *Dalton Trans.* **2009**, 2999–3008; b) S. Shimizu, A. Moriyama, K. Kito, Y. Sasaki, *J. Org. Chem.* **2003**, *68*, 2187–2194.

[14] For ring-opening reaction of isoxazoles using Fe/NH_4Cl see: a) Y.-G. Lee, Y. Koyama, M. Yonekawa, T. Takata, *Macromolecules* **2009**, *42*, 7709–7717; b) D. Jiang, Y. Chen, *J. Org. Chem.* **2008**, *73*, 9181–9183.

[15] a) M. Nishio, M. Hirota, Y. Umezawa, *The CH/π Interaction: Evidence, Nature and Consequence*, Wiley-VCH, NY, **1998**; b) O. Takahashi, Y. Kohno, M. Nishio, *Chem. Rev.* **2010**, *110*, 6049–6076.

[16] The relative quantum yields of fluorescence were determined by comparison of the integrated area of the emission spectrum of the samples with a reference of anthracene in EtOH ($\Phi = 0.27$). For the metal-free studies, calix[4]arenes **4** and **L** were prepared as 20 μM in MeOH/$CHCl_3$ (49:1, v/v). For the metal-bound studies, $AgClO_4$ (5 equivalents) were added to 20 μM calix[4]arenes **4** and **L** in MeOH/$CHCl_3$ (49:1, v/v). Emission spectra of these samples were integrated from 350 to 600 nm with excitation at 372 nm. The relative quantum yields were calculated with the equation: $\Phi = (A_{ref}/A) \times (F/F_{ref}) \times (n^2_{MeOH}/n^2_{EtOH}) \times \Phi_{ref}$, where A is the absorbance at the excitation wavelength, F is the integrated emission area, and n is the refractive index of the solvent ($n_{MeOH} = 1.3282$, $n_{EtOH} = 1.3640$ at 25 °C). Related references: a) D. F. Eaton, *Pure Appl. Chem.* **1988**, *60*, 1107–1114; b) W. R. Dawson, M. W. Windsor, *J. Phys. Chem.* **1968**, *72*, 3251–3260; c) F. I. El-Dossoki, *J. Chin. Chem. Soc.* **2007**, *54*, 1129–1137.

[17] For Job plot, please see: a) P. Job, *Ann. Chim.* **1928**, *9*, 113–203; b) K. A. Connors, *Binding Constants*, Wiley, NY, **1987**.

[18] H. A. Benesi, J. H. Hildebrand, *J. Am. Chem. Soc.* **1949**, *71*, 2703–2707.

[19] a) L. Fang, W. H. Chan, Y. B. He, W. J. Kwong, W. M. Lee, *J. Org. Chem.* **2005**, *70*, 7640–7646; b) J.-L. H. Jiwan, C. Branger, J.-Ph. Soumillion, B. Valeur, *J. Photochem. Photobiol. A* **1998**, *116*, 127–133.

[20] a) S. Shinkai, M. Ikeda, A. Sugasaki, M. Takeuchi, *Acc. Chem. Res.* **2001**, *34*, 494–503; b) M. Takeuchi, M. Ikeda, A. Sugasaki, S. Shinkai, *Acc. Chem. Res.* **2001**, *34*, 865–873; c) T. Nabeshima, S. Akine, *Chem. Rec.* **2008**, *8*, 240–251.

[21] We thank one of the reviewers for suggesting this method, which helped to elucidate the stepwise binding of **L** with 2 equivalents of Ag^+ ions. For stepwise metal ions binding, see: a) H. A. Michaels, C. S. Murphy, R. J. Clark, M. W. Davidson, L. Zhu, *Inorg. Chem.* **2010**, *49*, 4278–4287; and b) ref. [10c].

[22] The participation of the phenoxy rings of **L** in the cation–π interaction with Ag^+ ions can be proved by the downfield shifts of the *para*-aromatic protons on the calix[4]arene skeleton. As shown in Figure 6, the two sets of the *para*-aromatic protons merged at ca. 6.2 ppm (overlapped with H_b protons) before adding Ag^+, then were downfield shifted and separated into two sets of triplets at 6.97 and 7.51 ppm, respectively, by adding 2 equiv of Ag^+.

[23] The association constant was calculated by using a Stern–Volmer plot, see: B. Valeur, *Molecular Fluorescence: Principles and Applications*, Wiley-VCH, Weinheim, **2001**, p. 77.

[24] I. Leray, B. Valeur, *Eur. J. Inorg. Chem.* **2009**, 3525–3535.

Received: January 13, 2011
Published online: April 19, 2011

